J. Ind. Geophys. Union ( September 2016 )
**v.20, no.5, pp: 482-489**

# Assessing Quality of Masonry Dam using Seismic and Electrical Tomography

**M.S. Chaudhari*, M. Majumder, V. Bagade and S. Ranga**

Central Water and Power Research Station, Pune-411024, Maharashtra, India

*Corresponding Author: geophysics.cwprs@gmail.com

**ABSTRACT**

The ageing and degradation of dam structures is an inevitable problem and its consequences on the safety of the structure are important. Presently, site characterization using geotechnical engineering has some limitations to adequately describe the subsurface ground conditions. All geotechnical tests provide information from point to point and the values are interpolated in between places. These tests grossly under sample the subsurface and are frequently inadequate. Geophysical methods are useful as non-destructive tools that can provide information over large volumes as compared to point measurements. The use of seismic tomography and electrical resistivity imaging in the assessment of dam structure is very apt and useful. Seismic tomography survey was carried out in five horizontal and two vertical planes in the body of the Manikdoh masonry dam and one electrical resistivity imaging profile was taken on the top of the dam. The travel time data for tomography analysis was collected by placing geophones on the downstream face and hammer points on the upstream face of the dam. The compressional (P-) wave velocity distribution between each consecutive pair of source line and receiver line of the plane was computed using Simultaneous Iterative Reconstruction Technique. The weak zones, if present, reveal low P- wave velocity values and hence can be delineated. The reliability of travel time data is ensured by comparing the P- wave velocities at the point of intersection of common source to receiver pairs in horizontal and vertical planes. The tomography survey results revealed that the low velocity zones (velocity ranging between 1500 m/s to 2500 m/s) are between elevations 695 m to 705 m from chainage 463 m to 469 m. The four weak zones obtained from the horizontal planes matched well with that in vertical tomograms. Further, these low velocity zones are supported by presence of low resistivity patch (resistivity ranging between 129 Ω m to 829 Ω m) between elevation from 697 m to 693 m from chainage 462 m to 474 m in electrical resistivity imaging section.

**Key words:** Seismic tomography, dam safety, masonry dam, Imaging

## INTRODUCTION

Assessing the quality of dam structure is important to ensure its integrity and stability. Seismic Tomography has been used extensively in geophysical work (Dines and Lytle, 1979), e.g. for a dam site on Reunion Island (Cotton et al., 1986), for research on buried voids, for shafts and tunnels (Lytle and Dines, 1980) and for Pre-and Post-excavation studies for a nuclear power plant (Wadhwa et al., 2005). In tomographic reconstruction, seismic energy, which has propagated through a medium, is measured and from this energy, internal distribution of amplitude, phase shift or travel time observations (acoustic tomograms) are obtained by inversion process (Redington and Berninger, 1982; Jackson and Tweeton, 1994). Seismic tomography (using travel time data) and electrical tomography surveys were carried out in the present study for assessing the quality of a masonry Dam.

Manikdoh dam is a masonry dam with a height of 53 m and length of 927.05 m, constructed on River 'Kukadi' in Junnar Taluka of Pune District in the year 1984 which has a total storage capacity of 308.06 M.cum (10.88 TMC). Subsequent to the impoundment of the dam, heavy leakages were observed through the masonry in both the galleries as well as in the downstream face of the dam.

In view of this, seismic straight ray travel time tomography of the structure was carried out to suggest possible weak zones which are susceptible for seepage. Seismic tomography survey was carried out along five horizontal and two vertical planes in the month of May when the water level in the reservoir was minimum. The quality of in-situ masonry is an important parameter and can be assessed by seismic wave method as the compressional wave velocities evaluated by this technique give an idea of the strength of the masonry. The velocity distribution, in turn helps in delineating the lateral and vertical extent of weak zones by anomalous velocity values. Electrical Resistivity Imaging was carried out across one profile using 48 electrodes with 2 m spacing on the top of the dam.

## METHODOLOGY

### Seismic Tomography

Seismic wave tomography was carried out with the help of a 10 Kg Sledge hammer at preset locations on the upstream face of the dam while the seismic wave arrivals were picked up by different detectors (geophones of 10 Hz

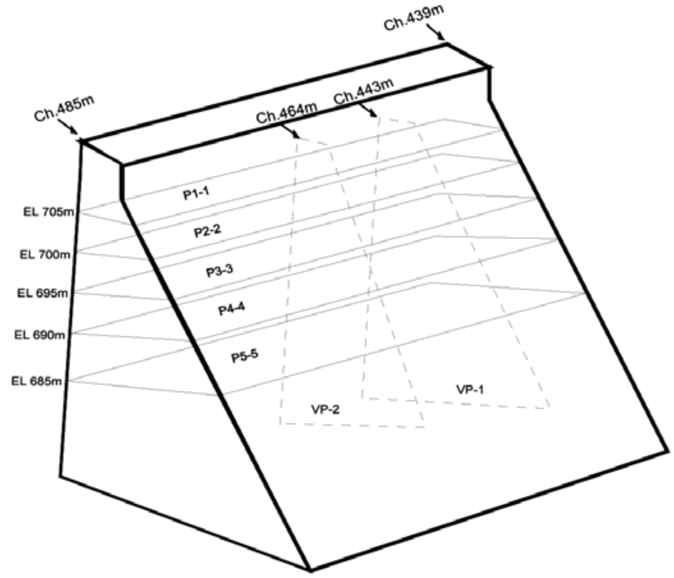


**Figure 1.** Schematic diagram showing horizontal and vertical planes covered by Seismic Tomography Survey

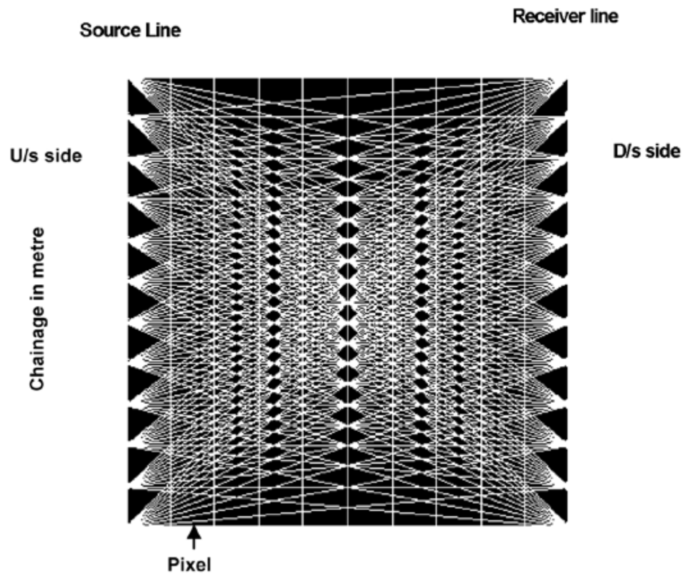


**Figure 2.** Typical ray diagram for various positions of source and receiver.

frequency) placed on the downstream face of the dam at known locations. The seismic arrivals were amplified and recorded on a 24-channel signal enhancement seismograph McSeis SX. The survey was conducted along five horizontal planes at elevations 705 m, 700 m, 695 m, 690 m, 685 m and two vertical planes at chainage 463 m and 443 m (Figure 1). The hammer points were located at the same elevation of geophones but on the upstream face of the dam. In horizontal planes, 24 geophones spaced 2 m apart were placed on the downstream face of the dam and 47 hammer points spaced 1 m apart were used for generating acoustic waves on the upstream face of the dam yielding 1128 ray paths. Typical ray paths between 12 positions of the hammer (source line) on the upstream face and 12 positions of geophones (receiver line) on the downstream face of the dam are shown in Figure 2. The first plane was at RL 705 m and other four planes were at 5 m elevation difference successively.

In vertical planes taken across the dam axis, 24 geophones spaced 1 m apart were placed on the downstream face of the dam and 24 hammer points spaced 1 m were used for generating acoustic waves on the upstream face of the dam yielding 576 ray paths. The geophones were planted vertically on the tip of the metallic rod inserted at the desired location by drilling small drill hole for maximum sensitivity.

**Table 1.** P-Wave velocity for different types of masonry (from Table 2 of Forde, and Batchelor, 1994)

| Sr. No. | Material | Av. Sonic Velocity (m/s) | Source |
|---|---|---|---|
| 1 | Granite masonry Pier no 1 | 3450 | Birjandi,1986 |
| 2 | Granite masonry Pier no 2 | 3370 | Birjandi,1986 |
| 3 | Red sandstone masonry Pier | 1970 | Birjandi,1986 |
| 4 | Yellow sandstone masonry Pier | 2040 | Birjandi,1986 |
| 5 | Whinstone masonry Pier | 2500 | Birjandi,1986 |
| 6 | White sandstone Pier | 1700 | Birjandi,1986 |

The travel times of these arrivals were measured from the seismic record on which a time scale is maintained. From the measured time of first arrival of the seismic waves and the distance between source (hammer point) and the receiver (geophone), the average velocity of propagation of the elastic wave for that distance was calculated. The recorded wave arrival data were analyzed by seismic ray tomography which enables the imaging of the velocity distribution within the sampled area. In this analysis, the area under study is divided into pixels, the number and size of which depend upon the number of ray paths and size of the area traversed. The data were analyzed using the algorithm of Jackson et al., (1992). From the velocity distribution, weak zones were delineated.

## Electrical Resistivity Imaging

The electrical resistivity imaging survey was conducted by ARES automatic resistivity imaging system on one profile with Wenner-Schlumberger array with 48 electrodes spaced at 2 m interval on the top of the dam from chainage 432 m to 526 m. The apparent resistivity values thus measured were inverted using RES2DINV software package to obtain true resistivity depth section.

## Data Analysis

Data analysis was done using ‘MIGRATOM’ (algorithm of Jackson et al., 1992) software. The seismic tomography of the dam across the zone between the receiver line on the downstream face and source line on the up-stream side of the dam which was divided into small pixel depending on the total number of P-wave arrivals recorded in the field experiment. The two dimensional plane 1-1 at elevation 705 m (Figure 1) between source line and receiver line was discretised on square grid points, 14 across the width of the plane (0.552m) and 47 along the plane (1.0 m). In the procedure adopted for data collection, there were 1128 rays and hence 1128 travel time equations. The number of pixels for this plane was 658. This means 658 unknowns against 1128 equations. It is possible to solve this type of problem through a near unique inversion. Once the pixel size is decided, tomographic inversion begins with an assumption of initial model of the P- wave velocity between source line and receiver line. With these initial average velocities, first arrival times of the rays for all possible positions of sources and receivers were calculated using straight ray tracings. These synthetic travel times were compared with the field measured travel times and the differences or residuals inverted to obtain perturbations to the velocity model using algorithm of Jackson et al., (1992). The procedure was repeated and the velocity model refined until, either there are no differences between the model travel times and the measured arrival times or RMS error was within the set limit (Singh and Singh, 1991). Travel time data for tomographic analysis was collected on one plane at a time.

The seven tomograms depicting P wave velocity distribution were obtained by inverting the arrival times. The reliability and uniqueness of the velocity tomograms were improved by taking the lower (1000 m/sec) and upper (4000 m/sec) limits of the velocities depending on wave velocities of different masonry reported in the literatures (Forde and Batchelor, 1994; Camplani et al., 2008) and are given in Table 1. Analysis of synthetic model studies suggests that the upper and lower velocity limits are helpful in obtaining a velocity distribution that is unique and matches more closely with the model data (Ghosh et al., 2000).

Resistivity imaging data analysis was done using RES2DINV software. The electrical resistivity depth section was obtained by plotting true resistivity values against depth. The electrical resistivity of saturated, unconsolidated sediment and rocks are controlled by porosity, grain size, morphology of pore space and resistivity of the pore fluid. The range of resistivities for the stone masonry is very large extending from 10 Ω m to 10000 Ω m (RILEM TC 127-MS, 2001). In the model studies carried out in saturated and dry rubble masonry (Flint et al., 1999) resistivity shows a variation from 200 Ω m to 2000 Ω m respectively.

## RESULTS AND DISCUSSION

## Seismic Tomography

The five horizontal and two vertical tomograms depicting lateral and vertical variations of P-wave velocities for the planes between source lines on the upstream side and

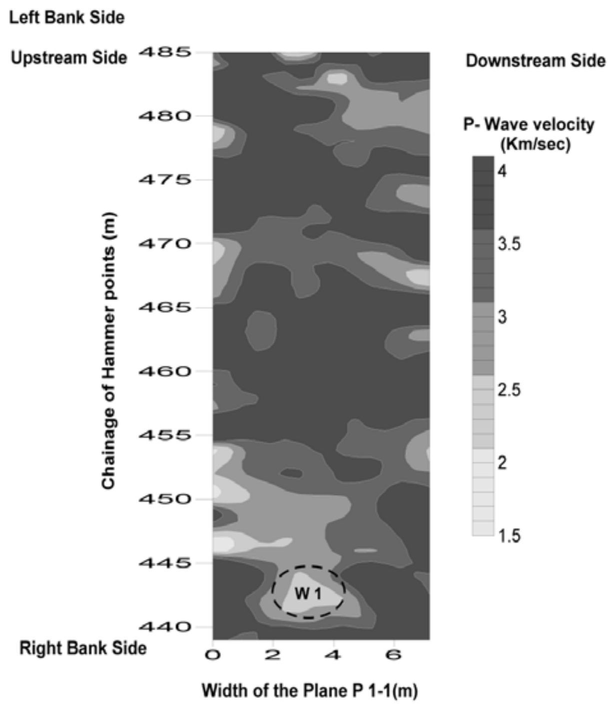


**Figure 3.** P- wave velocity distribution along plane P 1-1 (705-705) m elevation

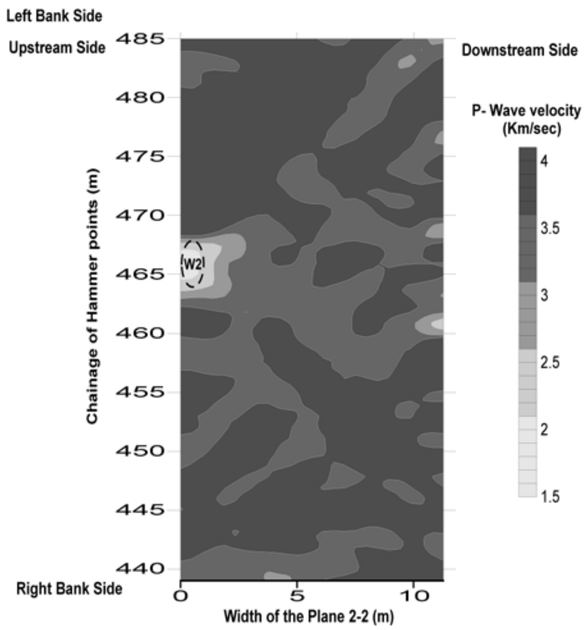


**Figure 4.** P- wave velocity distribution along plane P 2-2 (700-700)

receiver lines on the downstream side were obtained by inverting the arrival times using algorithm of Jackson et al., (1992).

During the analysis, the lower velocities observed very close to source and receiver lines were ignored. This is because these lower velocities may be due to ray density being less, close to the source and receiver locations or due to actual weak zones or their combinations. As it is not possible to separate the contribution of these factors, it is recommended that weak zones observed very close to the source and receiver locations be ignored. Tomograms depict contoured image of the P-wave velocities in grey scale, showing low velocity region in light grey colour and high velocity region in dark grey colour.

Figure 3 shows a low velocity zone W 1 with velocity range 2000 to 2500 m/sec observed from chainage 441 m to 444

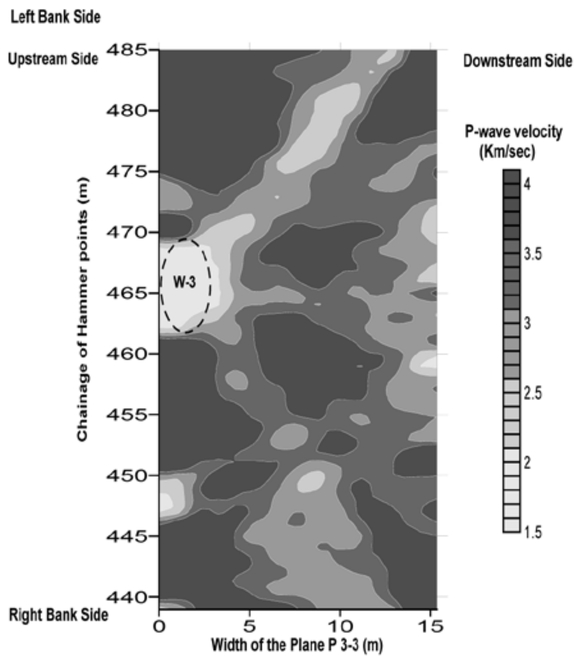


**Figure 5.** P- wave velocity distribution along plane P 3-3 (695 – 695)

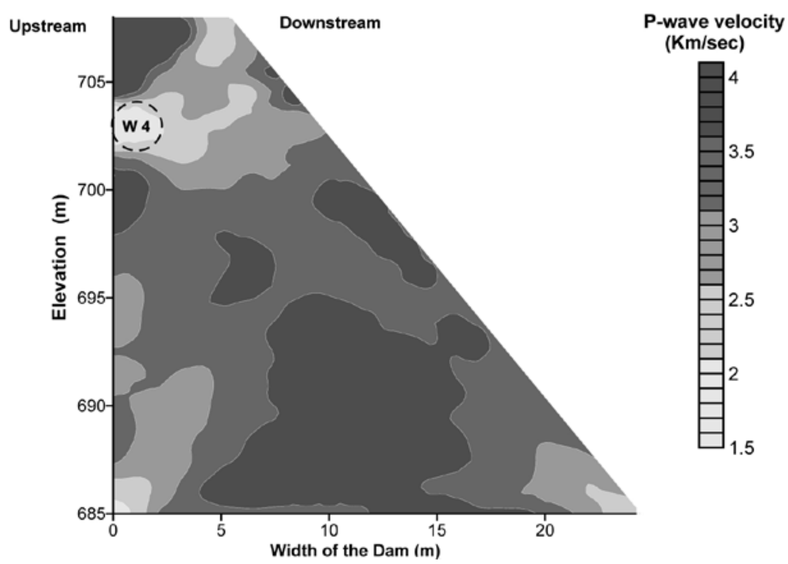


**Figure 6.** P- wave velocity distribution along vertical plane VP 1 at chainage 443 m

m on the upstream side extending from 2 m to 4.5 m across the plane 1-1. Similarly Figure 4 shows the P-wave velocity distribution for plane 2-2 at 700 m elevation. This plane appears to have a velocity above 2500 m/s. An isolated low velocity zone W 2 (velocity ranging from 1500 to 2500 m/sec) can however be spotted from chainage 463 m to 468 m on the upstream side and extending from 0 m to 2 m across the width of the plane.

P-wave velocity distribution for plane 3-3 at 695 m elevation is depicted in Figure 5. A very prominent low velocity zone W 3 with velocity ranging from 1500 m/sec to 2500 m/sec is observed from chainage 462 m to 469 m extending from 0 m upstream to 4 m towards downstream. The remaining part of the plane shows a velocity above 2500 m/s indicating good quality masonry.

P-wave velocity distribution for plane 4-4 at 690 m elevation and for plane 5-5 at 685 m elevation shows high values of P-wave velocity (ranging from 2500 m/s to 4000 m/s) indicating good quality masonry along the entire planes. So, no weak zone was attributed to these planes.

Figure 6 depicts the P-wave velocity distribution of vertical plane VP-1 at chainage 443 m spanning the

**Table 2.** Correlation of weak zones observed in different seismic tomograms taken at different section of the Dam

| Sl. No | Plane No | Weak Zones | Elevation (m) | Chainage (m) | Description |
|---|---|---|---|---|---|
| 1 | P 1-1 | W 1 | 705 | 441-444 | 2 to 4.5 m across the plane |
| 2 | P 2-2 | W 2 | 700 | 463-468 | 0 to 2 m across the width of the plane |
| 3 | P 3-3 | W 3 | 695 | 462-469 | 0 to 4 m across the width of the plane |
| 4 | VP-1 | W 4 | 702-705 | 443 | Extending laterally from 0 – 5m |
| 5 | VP-2 | W 5 | 700-703 | 463 | Dipping downwards to the downstream and tapering off at EL 697 m. |
| 6 | VP-2 | W 6 | 693-698 | 463 | Dipping downwards to the downstream and tapering off at EL 692 m. |

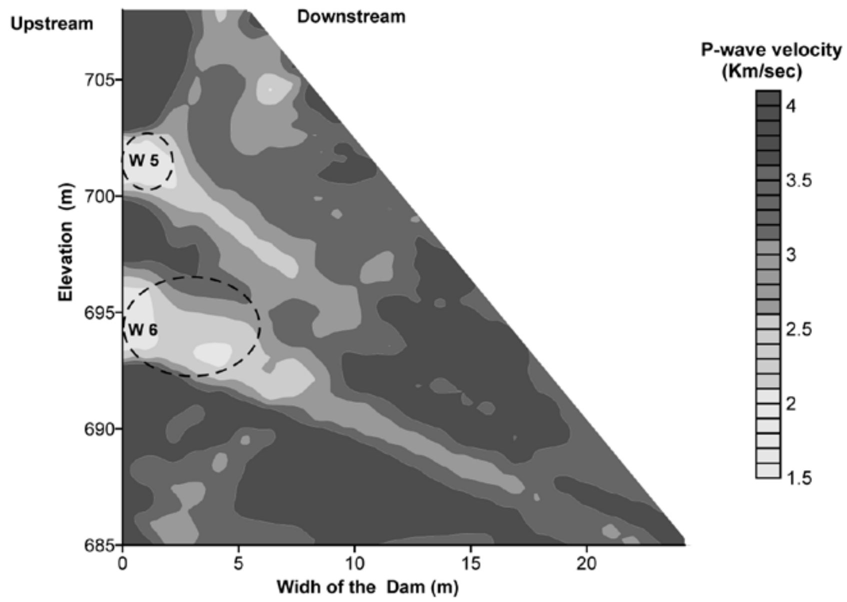


**Figure 7.** P- wave velocity distribution along vertical plane VP 2 at chainage 463 m

elevation range 685 m to 708 m. A low velocity zone W 4 with velocity ranging from 1500 m/s to 2500 m/s is seen from elevation 702 to 705 m and extending laterally from 0 m upstream to 5 m downstream. The rest of the plane shows velocities above 2500 m/s suggesting good quality masonry. This low velocity zone W 4 may be correlated with the low velocity zone W 1 found in plane P 1-1 (Figure 3) from chainage 441 m - 444 m at elevation 705 m.

Figure 7 depicts the P-wave velocity distribution of vertical plane VP-2 at chainage 463 m extending from elevation range 685 m to 708 m. Two low velocity zones with velocity ranging from 1500 m/s to 2500 m/s are seen on the upstream side. The first low velocity zone W 5 is spotted from EL 700 m to 703 m on the upstream side dipping down towards downstream and tapering off at EL 697.5 m extending 8 m towards downstream. The second low velocity zone W 6 is observed from elevation 693 m to 698 m at upstream face dipping down towards downstream and tapering off at elevation 692 m extending for 8 m from upstream to downstream.

## Electrical Resistivity Imaging

One electrical resistivity imaging section of 94.0 m length taken on the top of the dam at elevation 714.3 m from chainage 432 m to 526 m using Wenner-Schlumberger electrode configuration is shown in Figure 8. From the section it is seen that one low resistivity zone with resistivity ranging from 129 Ω m to 829 Ω m exists from chainage 462 m to 474 m corresponding to elevation from 700 m to 696 m. This low resistivity zone corroborates with the low velocity zone W 3 obtained in horizontal plane 3-3 at elevation 695 m.

## Correlation of weak zones

The correlation studies of low velocity zones observed in different tomograms indicates that the low velocity zone W 1 at Plane 1-1 (Figure 3) coincides with low velocity zone W 4 observed in Plane VP-1 (Figure 6) between elevation 702 m to 705 m and within chainage 441 m to 443 m.

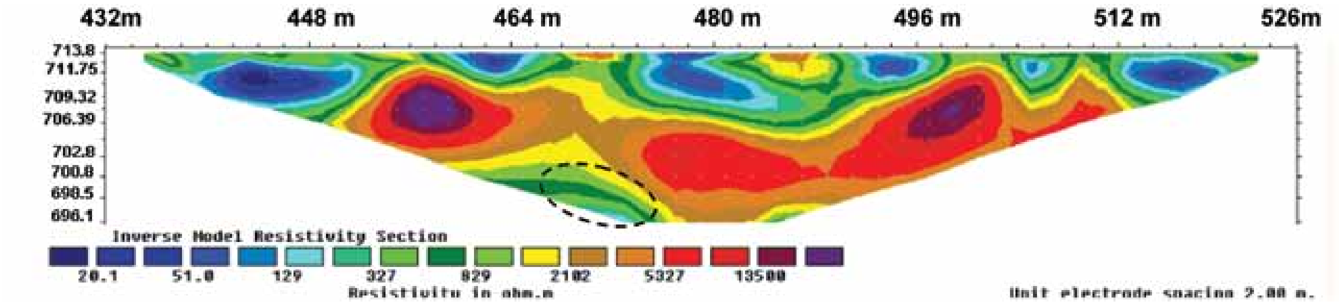


**Figure 8.** Electrical Resistivity Imaging Section from chainage 432 m to 526 m.

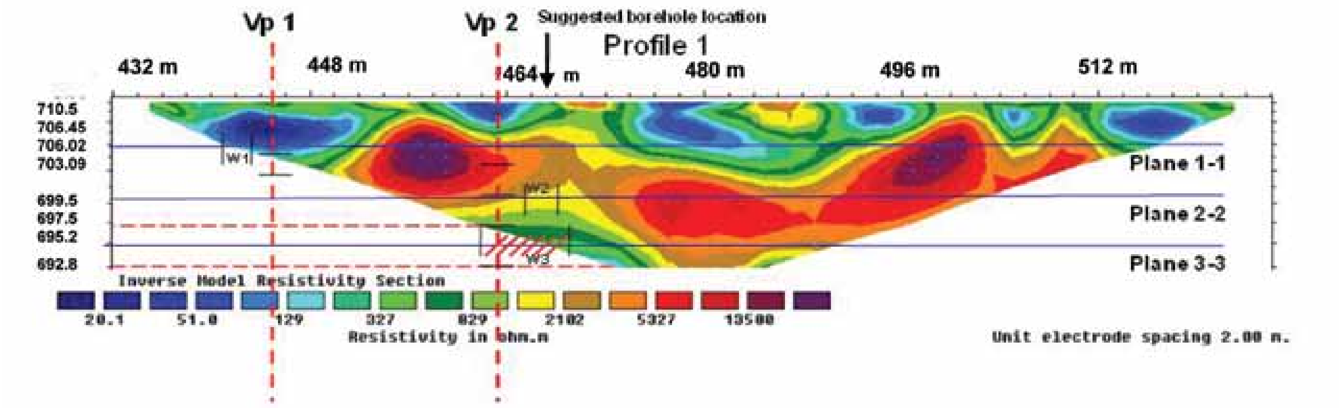


**Figure 9.** Correlation of Electrical Resistivity Imaging section with Seismic tomograms obtained at different elevations.

The correlated weak zone W 4 has a lateral extension of approximately 4 m. Further correlation indicates a weak zone of relatively greater extension at planes P 2-2, P 3-3 and VP-2.

The low velocity zone W 2 observed at Plane P 2-2 (Figure 4) occurring within chainage 463 m to 468 m can be correlated with the low velocity zone W 3 in plane 3-3 (Figure 5). These zones further can be correlated with two low velocity zones W 5 and W 6 observed in plane VP- 2 (Figure 7) at elevation between 693 to 703 m. The tabular presentation has been prepared for better view of correlation and is shown in Table 2.

Results obtained from seismic tomography survey were further compared with electrical resistivity imaging section of 94.0 m length taken on the top of the dam at elevation 714.3 m from chainage 432 m to 526 m (Figure 9). A relatively low resistivity zone with resistivity ranging from 129 Ω m to 829 Ω m has been observed from chainage 462 m to 474 m at elevation from 697 m to 693 m. This resistivity range corresponds to saturated masonry (RILEM TC 127-MS, 2001; Flint et al., 1999). This low resistivity zone also correlates with the low velocity zones W 2, W 3, W 4, W 5 found in tomograms of Plane 2-2, Plane 3-3 and vertical plane VP-2 respectively.

## CONCLUSIONS

The tomography survey results suggest that the possible low velocity zones lie between elevations 695 m to 705 m. Two low velocity zones W 2 & W 3 in the horizontal plane P 2-2 and P 3-3 are further supported by the low velocity zone W 5 and W 6 obtained from vertical section VP-2 at elevation 700 m to 703 m and 693 m to 698 m. Therefore, the prominent low velocity zone extending from elevation 695 m to 703 m from chainage 462 m to 469 m is inferred to be a weak zone. From the Electrical Resistivity Imaging section, it is observed that one low resistivity zone with resistivity ranging from 129 Ω m to 829 Ω m from chainage 462 m to 474 m at elevation from 697 m to 693 m corroborates with the low velocity zone W 2, W 3, W 4, W 5 found in tomograms of Plane 2-2, Plane 3-3 and vertical plane VP-2 respectively at elevation 695 m. These weak zones are susceptible for seepage and can be selectively treated.

## ACKNOWLEDGEMENTS

Authors are grateful to Dr. M. K. Sinha, Director, Central Water and Power Research Station (CWPRS), Pune for constant encouragement and for permission to publish this paper. The help and co-operation extended by project authorities during collection of data is thankfully acknowledged. Authors are thankful to Dr. M.R.K. Prabhakar Rao for useful suggestions. They also express thanks to B.V.S. Murthy for useful suggestions and editing.

## Compliance with Ethical Standards

The authors declare that they have no conflict of interest and adhere to copyright norms.

## REFERENCES

Birjandi, F. K., 1986. Sonic investigation of masonry structures, Ph.D. Thesis, University of Edinburgh.

Camplani, M., Cannas, B., Carcangiu, S., Concu, G., Fanni, A., Montisci, A., and Mulas, M. L., 2008. Acoustic Tomography for non destructive testing of stone masonry, Springer-Verlag Berlin Heidelberg, Part II, LNCS 5073, pp: 596-605.

Cotton, J.F., Deletie, P., Jacquet – Francillon, H., Lakshmanan, J., Lemeine, Y., and Sanchez, M., 1986. Curved ray seismic tomography: Application to the Grand Etang Dam (Reunion Island), First break, v.4, pp: 25-30.

Dines, K.A., and R.J. Lytle, 1979. Computerized geophysical tomography, IEEE Proc., v.67, pp: 1065-1073.

Flint, R. C., Jackson, P. D., and McCann, D. M., 1999. Geophysical imaging inside masonry structures, NDT&E international, v.32, pp: 469-479.

Forde, M. C., and Batchelor, A. J., 1994. Digital Impulse Radar and sonic testing of bridges, Proceedings of the Symposium on the Application of Geophysics to Engineering and Environmental Problems (SAGEEP), Boston, Massachusetts, pp: 319-341.

Ghosh, N., Wadhwa, R.S., and Mukhopadhyay, R., 2000. Seismic Tomography of synthetic models and Masonry dam. Third International Research and Development Conference on Sustainable Development of Energy Resources, pp: 87-95.

Jackson, M.J., Tweeton, D.R. and Fridel, M.J., 1992. Approaches for optimizing the use of available information in cross-hole seismic tomographic reconstruction, Proc. Geotech. Geocomputing Conference, Denver, pp: 130-143.

Jackson M. J., and Tweeton D. R., 1994. MIGRATOMGeophysical tomography using wavefront migration and fuzzy constraints, ISSN 1066-5552, Bureau of mines, United States department of the interior.

Lytle, R.J., and Dines, K.A., 1980. Iterative ray tracking between boreholes for underground image reconstruction, IEEE Trans, Geosci, Remote Sensing, V.GE -18, pp: 234-240.

Recommendations of RILEM TC 127-MS: Non-destructive tests for masonry materials and structures, Materials and Structures, 2001, v.34, pp: 134-143.

Redington, R.W., and Berninger, W.H., 1982. Medical Imaging Systems, Physics Today, v.34, no.8, pp: 36-46.

Singh, R.P., and Singh, Y.P., 1991. RAYPT A new inversion technique for geotomographic data, Geophysics, v.56, pp: 1215-1227.

Wadhwa, R.S., N., Ghosh, Chaudhari, M.S., Subbarao, Ch., and Mukhopadhyay, R., 2005. Pre and Post-excavation cross-hole seismic and geotomographic studies for a nuclear power project, Journal of Indian Geophysical Union, v.9, no.1, pp: 137-146.